Fundamental studies on enhancement and blinking mechanism of surface-enhanced Raman scattering (SERS) and basic applications of SERS biological sensing

4 **AUTHORS**, INCLUDING:

Yuko S Yamamoto

Kagawa University

23 PUBLICATIONS   122 CITATIONS

SEE PROFILE

Yukihiro Ozaki

Kwansei Gakuin University

916 PUBLICATIONS   17,729 CITATIONS

SEE PROFILE

Tamitake Itoh

National Institute of Advanced Industrial Sc…

105 PUBLICATIONS   2,207 CITATIONS

SEE PROFILE

REVIEW ARTICLE

Fundamental studies on enhancement and blinking mechanism of surface-enhanced Raman scattering (SERS) and basic applications of SERS biological sensing

Yuko S. Yamamoto[1], Mitsuru Ishikawa[2], Yukihiro Ozaki[3], Tamitake Itoh[1,†]

[1] *Nano-Bioanalysis Research Group, Health Research Institute, National Institute of Advanced Industrial Science and Technology (AIST), Takamatsu, Kagawa 761-0395, Japan*

[2] *Department of Chemistry, Josai University, Itado, Saitama 350-0295, Japan*

[3] *Department of Chemistry, School of Science and Technology, Kwansei Gakuin University, Sanda, Hyogo 669-1337, Japan*

Corresponding author. E-mail: †tamitake-itou@aist.go.jp

We review recent our results in the fundamental study of surface-enhanced Raman scattering (SERS) with emphasis on experiments that attempted to identify the enhancement and blinking mechanism using single Ag nanoparticle dimers attached to dye molecules. These results are quantitatively discussed in the framework of electromagnetic mechanism. We also review recent our results in basic SERS applications for biological sensing regarding detections of cell surface molecules and distinction of disease marker molecules under single cell and single molecule level.

Frontiers of Physics

Contents

1 Introduction

Nanostructures and nanoparticle (NP) aggregates of plasmonic metals (e.g. Ag and Au) generate strong enhancement of Raman scattering intensity from molecules adsorbed on their surfaces. This phenomenon is widely known as surface-enhanced Raman scattering (SERS) [1–4]. In particular, huge enhancement factors of SERS (10^{10} to 10^{14}) from molecules located in the NP gaps of aggregates allow us to sensitively measure spectra of analytes at single molecule (SM) level [5–9]. The high-sensitivity and selectivity of SERS motivate researchers to extend its application towards biosensing [10–13]. However, despite the significant impact of SERS in basic research, fundamental issues such as lack of conclusive experimental evidence for validating the mechanism underlying the enhancement and blinking have prevented us from clear understanding of SERS, and furthermore difficulty in finding out potential SERS applications limits its public recognition.

It is proposed by many researchers that there are two

enhancement mechanisms of SERS [3, 14]. These two mechanisms are called the electromagnetic mechanism (EM) and the chemical mechanism, respectively. The EM mechanism is characterized by twofold plasmonic EM field enhancement of Raman scattering signals from molecules adsorbed on plasmonic metal NPs or NP aggregates [3, 7, 14–20]. Chemical mechanism is characterized by shifting of Raman scattering in non-resonance to that in resonance through the formation of charge transfer complexes between adsorbed molecules and metal surfaces [2, 21–25]. Both mechanisms have been experimentally investigated in detail and have been found to be correct [16, 22, 23, 26–28]. Accordingly quantitative evaluation of SERS based on exclusive one mechanism is important in an effort to find out which mechanism is dominant. EM mechanism has universality for every molecular specy. Thus, we have investigated the origin of enhancement and blinking in the framework of EM mechanism. Based on the mechanism we have studied SERS biosensing regarding detections of cell surface molecules and distinction of disease marker molecules to explore the real application of SERS [29–34].

In the present mini-review, we focus our attention on two topics below in SERS studies. First, in Section 2, we summarize results of our recent experimental investigations to validate EM mechanism by quantitatively evaluate enhancement factors of SERS [16, 35]. Microspectroscopy using single Ag NP dimers enables us to quantitatively evaluate SERS spectra by EM mechanism excluding inhomogeneity induced by NP dimer-by-dimer variations in SERS spectra [16, 35, 36]. Ag NP dimers, whose nano-gaps are the minimum unit generating SM SERS, directly illustrate relationship among the enhancement factors, SERS spectra and plasmon resonance spectra by comparing with shapes of Ag NP dimers [37]. The relationship provided us not only quantitative verification of EM mechanism in SERS but also mechanism of SERS blinking as an extension of EM mechanism [38]. Second, in Section 3, we explored basic applications of SERS using four types of biological targets; yeast, helicobacter pylori, E. coli, and hemoglobin A1c, as potentially being incorporated to future progress in SERS biosensing [29–34]. The equipment used in the section is common to that for studies on EM mechanism as a platform so that we succeeded to identify the molecular species of proteins generating SERS signals on living single yeast cell wall at single molecular level. In this section we also briefly summarize the advantages of SERS over fluorescence spectroscopy for label-free detection of biomolecules by taking examples from our own investigations. Finally, in conclusion, we correlate our recent findings with potential applications of SERS.

2 Enhancement and blinking of SERS quantitatively evaluated by EM mechanism

2.1 Introduction

In this section, we describe EM mechanism of SERS and quantitatively demonstrate its absolute validity. Ag NP dimer-by-dimer variations are well-explained by the selective enhancement of SERS bands whose maxima are close to the plasmon resonance maxima through second EM enhancement, that is, coupling of plasmon resonance and Raman light [16]. Experimental observations of plasmon resonance, SERS, and shapes of the Ag NP dimers were compared with FDTD (Finite-difference time-domain) calculations, which enable us to reproduce spatial and spectral distribution of EM fields around Ag NP dimers [16]. The experimental enhancement factors were quite consistent with the calculations, indicating that EM mechanism has dominant role in SERS. Thus, we applied EM mechanism to evaluate SERS blinking [38].

2.2 Two-fold EM enhancement in SERS evaluated by EM mechanism

To quantitatively evaluate the EM mechanism, we have examined two types of experimental observations: (i) Ag NP dimer-by-NP dimer variations in SERS spectra [35]; (ii) Quantitative evaluation of SERS spectra based on EM mechanism [16].

We explain here an theoretical outline of the EM mechanism. A Raman process is composed of an excitation and an emission process. In these processes, a molecule and a field exchange light energy. The rates of the exchange are enlarged by increasing in local mode density of the field in the vicinity of plasmonic metal NPs because of their large conduction electron density and their long oscillation time. Thanks to the increasing in local mode density, both Raman excitation and emission process become efficient. In other words, Raman excitation obtains the enhancement due to coupling of incident light with plasmon, which is called first EM enhancement [15, 17], and Raman emission obtains that due to coupling of Raman light with plasmon, which is called second EM enhancement [15, 17]. Note that a broad plasmon resonance line width (∼200 meV) enables EM enhancement to work on both Raman excitation and the Raman emission transition rates of a molecule. The highest enhancement factors of SERS are theoretically and experimentally observed for molecules located at junction of metal NP dimers. The factors are up to 10^{10-14}, allowing us to

measure SERS spectra at SM level.

The twofold EM enhancement provides us with a simple expression for total SERS enhancement because it is a product of EM enhancement of the incident and scattered light coupled with plasmon. Thus, the total enhancement factor M_{EM} of SERS is given by [15, 17]

$$
\begin{aligned}
&|M_{\mathrm{EM}}(\lambda_{\mathrm{L}}, \lambda_{\mathrm{L}} \pm \lambda_{\mathrm{R}})|^2 \\
&= \left| \frac{E^{\mathrm{Loc}}(\lambda_{\mathrm{L}})}{E^{\mathrm{I}}(\lambda_{\mathrm{L}})} \right|^2 \times \left| \frac{E^{\mathrm{Loc}}(\lambda_{\mathrm{L}} \pm \lambda_{\mathrm{R}})}{E^{\mathrm{I}}(\lambda_{\mathrm{L}} \pm \lambda_{\mathrm{R}})} \right|^2 \\
&= |M_1(\lambda_{\mathrm{L}})|^2 \times |M_2(\lambda_{\mathrm{L}} \pm \lambda_{\mathrm{R}})|^2
\end{aligned} \tag{1}
$$

where E^{Loc} and E^{I} is localized and incident EM field amplitude, respectively. M_1 and M_2 are first and second EM enhancement, respectively. λ_{L} and $\lambda_{\mathrm{L}} \pm \lambda_R$ are excitation light and Raman light wavelength, respectively. More details in the Eq. (1) have been provided elsewhere [36]. It is not difficult to understand $|M_1|^2$ because it is increment in Raman excitation EM field intensity by plasmon resonance, but not so for $|M_2|^2$. Thus, demonstration of $|M_2|^2$ is a key to understand "twofold" EM enhancement. The important point is that the spectrum of $|M_2|^2$ is expected to be similar to that of plasmon resonance because the second enhancement is produced by scattering of Raman light through plasmon resonance [15, 17]. Thus, to experimentally evaluate two-fold EM enhancement, we identified the second EM enhancement factor $|M_2|^2$ as dependence of SERS spectra on plasmon resonance maxima.

We summarize here how we experimentally evaluated $|M_2|^2$. It is difficult to identify $|M_2|^2$ as dependence of SERS spectra on plasmon resonance maxima, because EM fields on larger Ag NP aggregates are complex due to overlapping between dipolar and multipolar plasmonic EM fields and the overlapping may break optical reciprocity. This difficulty can be resolved by selecting Ag NP aggregates which mainly show dipolar plasmon resonance exclusively coupled with SERS. Such Ag NP aggregates satisfy the following two criteria: (i) Polarization dependence of a plasmon resonance maximum follows a cosine-squared law, (ii) SERS maxima and plasmon resonance maxima have the same polarization dependence to each other [16]. We experimentally confirmed that Ag NP aggregates satisfying such criteria are always dimers when plasmon resonance maxima located around 600–680 nm [16]. We detected Ag NP dimer-by-dimer variations of SERS spectra of rhodamine 6G (R6G) molecules ($\sim 10^{-8}$ M) based on the criteria and the variations well explained in terms of the dependence of plasmon resonance spectra [35]. The explanations mean that EM mechanism certainly exists in SERS. The result motivates us to quantitatively reproduce SERS spectra also

by EM mechanism. SERS spectra from single Ag NP dimers were evaluated to determine one-to-one relationship among plasmon resonance, SERS, and the shapes of the dimers measured by scanning electron microscopy (SEM). The experimental observations were compared with FDTD calculations of the EM field induced by plasmon resonance using individual shapes of the dimers. The experimental enhancement factors of SERS $\sim 10^9$ were well consistent with that of the calculations within a factor of ~ 2. The consistency fortifies the indispensible importance of EM mechanism in SERS [35, 37].

2.3 SERS blinking quantitatively treated by EM mechanism

We discuss here the origin of SERS blinking based on EM mechanism. Blinking is well known as intrinsic fluctuation and intermittent of emission light from single quantum systems, e.g. quantum dots, single-molecular detections including SERS. SERS blinking has extensively been studied for more than a decade by various approaches [5–7, 39, 40]. Here representative "blinking mechanisms" for SERS are briefly summarized: molecules activated to metastable nonabsorbing and nonemissive states [41, 42], the molecules in thermal diffusion in-and-out of hot spots [43], molecules in thermal diffusion on the nanoparticle surface coupled with photo-induced electron transfer, the structural relaxation of surface active sites [44], thermally-stimulated molecular reorientation and chemical process [45], photoionization via charge-transfer states [46], and the morphology rearrangement of the metallic substrate [47].

However, analyses of SERS blinking in the previous works are limited to qualitative approaches. Complexity in the blinking mechanisms including unclear SERS mechanism prevent us from examining direct correlation between blinking and its origins. Thus, we quantitatively analyzed SERS blinking in terms of intensity and spectral instability based on EM mechanism under the common experimental conditions. In short, we selected Ag NP dimers adsorbed to R6G as a target molecule to exclusively analyze blinking by EM mechanism [38].

For quantitatively analysis in SERS blinking, we selected Ag NP dimers based on the criteria [16] and measured SERS, surface-enhanced fluorescence (SEF), and plasmon resonance spectra. Ag NPs were prepared by the Lee and Meisel method [48] and added NaCl (10 mM) and R6G ($\sim 10^{-8}$ M) to form SERS-active Ag NP aggregates. The R6G-adsorbed Ag NP aggregates including dimers were randomly immobilized onto a glass plate by spin-coating. A green laser beam from a cw Nd^{3+}:YAG laser (532 nm) was introduced as a light source of SERS

Yuko S. Yamamoto, et al., Front. Phys., 2014, 9(1)

33

and SEF. Plasmon resonance spectra coming from each Ag NP dimer were measured under dark-field condenser using white-light from a 50-W halogen lamp as described in Ref. [49]. The morphology of each Ag NP dimer was obtained using SEM. To add fluctuations which induce SERS blinking on Ag NP dimers, we used 1064-nm laser pulses from a cw Nd^{3+}:YAG laser. Further detailed experimental condition has been described in the report [38].

Here we outline EM enhancement factor of SEF M_{SEF}. M_{SEF} includes M_{EM}, which is shown in Eq. (1), and additionally includes an enhancement factor of the decay rate M_d for a molecule in the excited state due to resonance energy transfer from a molecule to a Ag dimer. Thus,

$$
\begin{aligned}
&|M_{SEF}(\lambda_L, \lambda_L \pm \lambda_R)|^2 \\
&= \frac{|M_1(\lambda_L)|^2 \times |M_2(\lambda_L \pm \lambda_R)|^2}{|M_d(d_{eff})|^2} \\
&= \frac{|M_{EM}(\lambda_L, \lambda_L \pm \lambda_R)|^2}{|M_d(d_{eff})|^2}
\end{aligned} \tag{2}
$$

where d_{eff} is effective distance between a molecule and a metal surface. More details in the Eq. (2) have been provided elsewhere [38]. To quantitatively confirm the origin of SERS blinking, we selected SERS and SEF active Ag NP dimers. Figures 1(a1)–(a3) shows Ag NP aggregates showing dipolar plasmon resonance whose maxima located around 600–680 nm. As indicated in the previous section such Ag NP aggregates generating detectable SERS and SEF spectra like Figs. 1(b1)–(b3) were always dimers as Figs. 1(c1)–(c3) [16]. We evaluated plasmon resonance and shapes of 12 Ag NP dimers that show SERS and SEF activity then calculated plasmon resonance and SERS spectra by FDTD calculation based on EM mechanism. These calculated spectra are quantitatively consistent with experimental ones as described [16].

SERS blinking means both drastic spectral changes and total intensity changes, meaning temporal spectral intensity instability in SERS. To quantitatively analyze the temporal spectral instability, we examined spectral changes in SERS and SEF for the same Ag NP dimer and theoretically restructured these spectra using
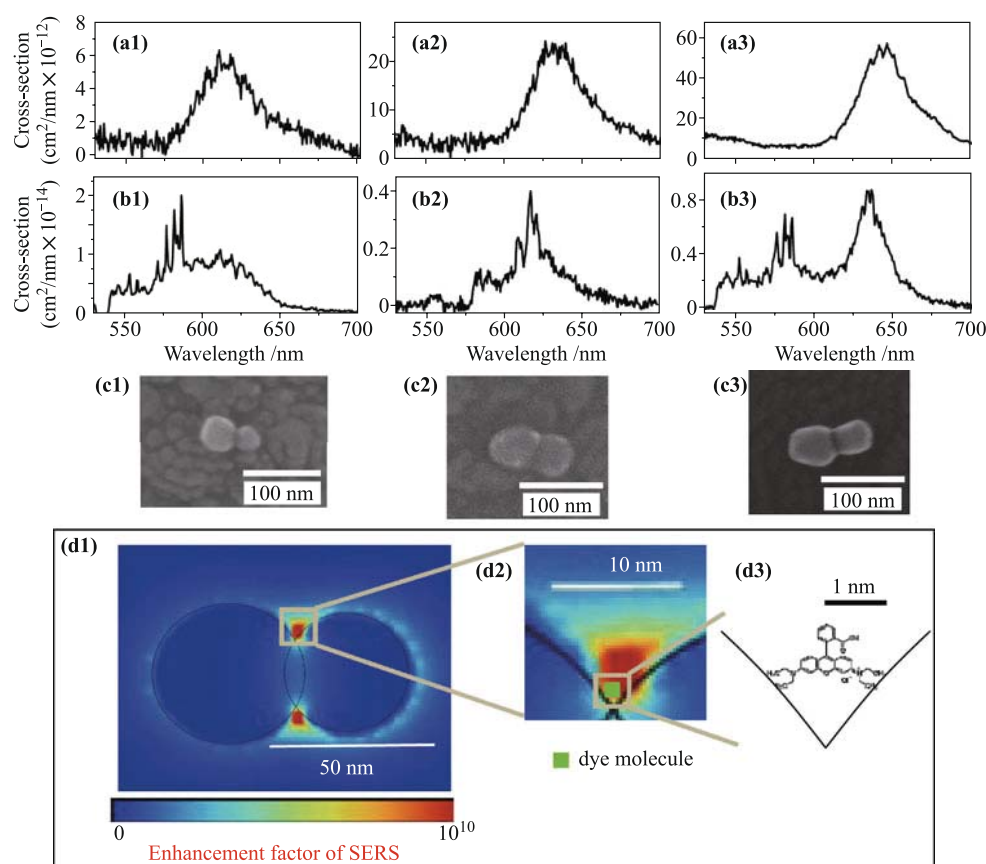

Fig. 1 Fundamental observation from Ag NP dimer adsorbed by R6G: (a1)−(a3) spectra of plasmon resonance, (b1)−(b3) those of SERS and SEF, and (c1)−(c3) SEM images obtained from three Ag dimers. Model for a Ag dimer generating SERS: (d1) electric field distribution around a Ag dimer calculated by FDTD, (d2) enlarged image of a crevasse in the Ag dimer, and (d3) assumed location of a R6G molecule at the crevasse. Reproduced from Ref. [38].
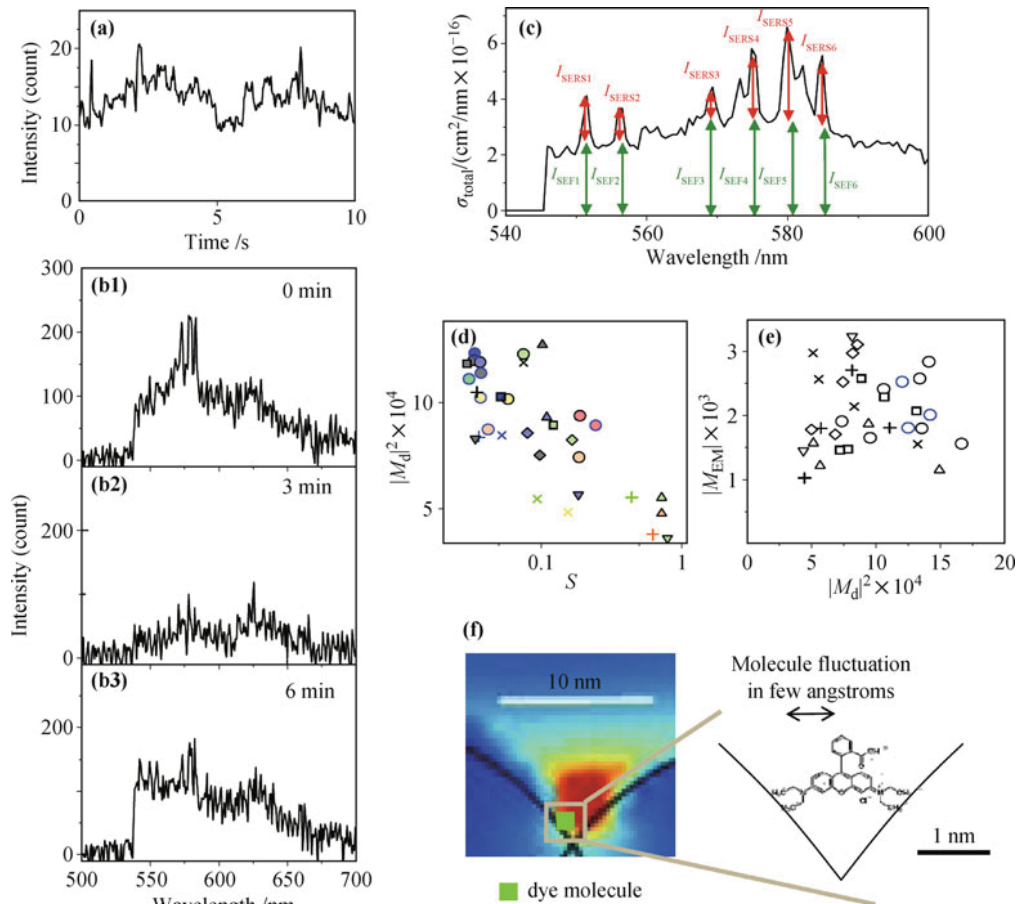
Fig. 2 Origin of SERS blinking: **(a)** Temporal profile of SERS intensity blinking including SEF blinking from a representative SERS generated from an Ag NP dimer. Intensity is integrated from 540 to 700 nm, **(b1)−(b3)** spectral changes in SERS and SEF from the common Ag dimer in (a), time lapse for each measurement is indicated in each panel. Exposure time for spectral detection is 5 s, **(c)** definition of SERS and SEF intensities along wavelength for analysis of S (normalized standard deviation scores of blinking) dependence of $|M_d|^2$ in SERS fluctuated region, **(d)** S dependence of $|M_d|^2$ in fluctuated region for eight dimers, **(e)** $|M_{EM}|$ dependence of $|M_d|^2$ for the eight dimers, **(f)** schematic of the origin of SERS and SEF blinking. Reproduced from Ref. [38].

EM mechanism. Figure 2 shows the summary of the analysis [38]. Figure 2(a) shows temporal total intensity instability in both SERS and SEF from a Ag dimer. Figures 2(b1)–(b3) show temporal spectral instability in SERS and SEF. Figure 2(c) indicates definition of SERS and SEF intensities. Using the definition, we can experimentally derive $|M_{EM}|$ and $|M_d|^2$ [38]. We quantified the intensity instability in SERS by normalized standard deviation scores (S) dependence of $|M_d|^2$. Regarding that $|M_d|^2$ is sensitive to effective distance between a molecule and a metal surface d_{eff} [38], S dependence of $|M_d|^2$ shown as Fig. 2(d) indicates that the instability is induced by the increasing in d_{eff}. $|M_{EM}| \ll |M_d|^2$ shown as Fig. 2(e) is reasonable, because $|M_{EM}|$ induced by radiative plasmons and $|M_d|^2$ induced by both radiative and nonradiative plasmons. Regarding that $|M_d|^2$ is more sensitive to d_{eff} than $|M_{EM}|$, the instability may be

a main fluctuation in SEF. Figure 2(f) shows a schematic of origin of SERS instability as a molecular fluctuation within several angstroms [38].

In short, experimental evaluation of changes in EM enhancement factor spectra has been demonstrated along the changes in plasmon resonance, explaining spectral instability in SERS and SEF spectra. The quantitative analysis reveals two new physical insights into blinking as follows. (i) The intensity instability is inversely proportional to the enhancement factors of decay rate of molecules. The estimation using the proportionality suggests that intensity instability is induced by fluctuations in separation of the molecules from Ag NP surfaces by several angstroms. (ii) The spectral instability is induced by blue-shifts in EM enhancement factors, which have spectral shapes similar to the plasmon resonance (data shown in Ref. [38]). This analysis provides us a quantita-

tive picture for intensity and spectral instability in SERS and SEF within the framework of EM mechanism. The work reveals that SERS blinking is quantitatively clarified by EM mechanism. Note that in the case of non-resonant molecules, the effect of EM mechanism for the SERS blinking activity is unclear. However, we comment that following three points may be the keys for determining the blinking activity of non-resonant molecules: (i) more confined hotspots are required to obtain higher EM enhancement from non-resonant molecules so that non-resonant molecules may be more sensitive to molecular fluctuation than resonant molecules, (ii) SERS blinking is expected to be smaller for non-resonant molecules because of weaker contribution of SEF fluctuation, and (iii) forming CT complexes will give weaker SERS blinking.

We note that the evaluation does not mean that the instability in SERS and SEF can be totally explained by EM mechanism excluding other ones composed of other system, e.g. Ag NPs and pyridine molecules showing strong chemical effect [28, 50]. We also underline that the current work does not identify the exclusive origin of blinking. The point is that blinking is correlated with the photo-excitation/emission mediated with the plasmon resonance [38]. The fact therefore suggests that the underlying reason for blinking is a photo-induced effect, such as thermal heating, photo-bleaching, or photo-induced diffusion, rather than purely chemical effects in the case of the system composed of Ag NPs and R6G molecules. We need further evaluation in SERS blinking to clear the exclusive origin of blinking in each system and we also believe our recent studies give help for further investigation.

2.4 Summary

We have quantitatively investigated the EM mechanism of SERS and demonstrated its absolute validity [16]. The intensity and spectral instability in SERS and SEF were also quantitatively analyzed. Experimental evaluation of SERS blinking revealed that changes in molecular locations and plasmon resonance cause intensity and spectral instability in SERS spectra, respectively. The present work reveals that fluctuation in SERS including blinking is quantitatively clarified by EM mechanism [38]. However, the present evaluation does not mean that the SERS enhancement mechanism can be totally explained by EM mechanism excluding other ones because we selected Ag NPs/R6G system to quantitatively evaluate the phenomena of SERS by only one mechanism. In particular SERS blinking, we believe the present achievement could help us to evaluate the degree of other mechanisms.

3   Applications of SERS to biological sensing

3.1   Introduction

A large number of reviews and articles on various applications of SERS to biological sensing have been published [51–98] including biomedical applications [51–62], cellular probing [63–68], in vivo cell probing [69–79], in vitro cell analysis [80, 81], imaging of individual cells [82, 83], differentiating cancer cells [84], imaging of proteins [85–88], bacteria detection [89–93], virus detection [89–93] and etc. These researches have mainly been carried out using confocal Raman microscopic systems under non-resonant Raman excitation conditions. The standpoints of our SERS applications compared with others are use of simple non-confocal Raman microscopic systems, resonant Raman excitation conditions, and plasmonic imaging with dark-field microscopy. The standpoints enable us to easily measure resonant SERS images at single molecule conditions checking adsorption of plasmonic metal nanoparticles on samples; for example, we succeeded to identify proteins generating SERS signals from single Ag NP dimers on living single yeast cell wall at single molecular level.

In this section, we briefly summarize the advantageous point of SERS for label-free detection of biomolecules over fluorescence spectroscopy. Our resent progresses in SERS applications for biological sensing using four types of biological targets; yeast, *helicobacter pylori*, E. coli, and Hemoglobin A1c (HbA1c) are also introduced here.

3.2   Advantages of SERS for biosensing

For the analysis of single biomolecules, fluorescent labels, such as dye molecules or quantum dots, have been well developed [100]. However, photobleaching or pH-dependence of such labels still prevents us from stable and long-time observation. Raman spectroscopy has certain advantages because the vibrational bands especially in the fingerprint region are sharper than fluorescence ones. The use of fluorescent tags is suffered from confused overlapping fluorescence spectra, which are broader than Raman spectra. Non-uniform photobleaching rates of each fluorescent tags also lead us to several potential complications [10]. Thus, Raman spectroscopy is useful for well-defined discrimination of molecular species including biomolecules. However, cross-sections of Raman scattering ($\sim 10^{-30}$ cm^2) is quite low compared with absorption cross-sections of fluorescence ($\sim 10^{-16}$ cm^2) so that there is a problem of sensitivity in Raman spectroscopy for biosensing [44]. SERS resolves the problem

by signal enhancement factors of 10^{10}–10^{14}. Thus, SERS has certain advantages for characterizing biomolecules over fluorescence spectroscopy and is now extensively explored for probing and analyzing intracellular and extracellular components.

3.3 Applications of SERS to cell sensing

One of the most effective bio-applications in SERS is cell sensing. Thanks to the demonstration of single molecule SERS, in recent years biomedical applications of SERS have become a subject with a variety of challenges and opportunities for practitioners of chemical engineering, applied biology, and medical field [51–99]. High enhancement factors of SERS also give us expectation on detailed analysis of proteins, sugar chains, and lipids on the cell wall at single or few-molecule level.

To detect cell surface molecules using SERS, adding pre-synthesized Ag NPs onto cell wall is the simplest way. However, affinity of molecules for Ag surfaces is a primary requirement for accomplishing large enhancement by forming Ag NP aggregates including the molecules.

Over the last few years we focused our research interests on SERS biosensing into: (i) *in situ* detection of biomolecules e.g. proteins on cell surfaces at single-molecular level; (ii) identification of plasmon resonance spectra and SERS spectra generating from each Ag nanoaggregate to analyze biomolecules on cell surfaces at single-molecular level. We start here to describe the study on yeast cells, which cell wall has affinity for Ag surface, showing potentials of SERS measurement for single molecular detection of cell surface molecules. Then we propose our solution using a method of Ag NPs photoreduced on cell surfaces for applying SERS to cells *Helicobacter pylori* and E.coli, whose surfaces do not have affinity for Ag surface.

We firstly selected yeast (*Saccharomyces cerevisiae*) cells for a target of bio-analysis. Yeast cells are important because they are one of the most extensively studied model eukaryotic organisms from genetics to biochemistry [101]. To understand surface interfacial chemistry and membrane protein dynamics in living yeast cells, we expect SERS to be analysis tool with single or a few molecules sensitivity. Figures 3(a) and (b) shows dark field images of living yeast cells without and with Ag NPs, respectively. Fortunately Ag NPs have certain affinity to the cell wall of yeast. Colored spots on the cells in Fig. 3(b) correspond to isolated Ag NPs or NP aggregates confirmed by AFM measurements [Fig. 3(c)]. Figures 4(a) and (b) shows blinking of SERS spots on a living single yeast cell and their SERS spectra, respectively. SERS blinking is the strong evidence of single or
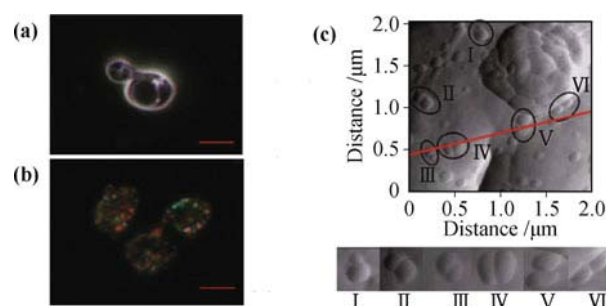

Fig. 3 Adsorption of Ag NPs on yeast cell surfaces: **(a)** Dark field image of yeast cells without Ag NPs (× 100 objective), **(b)** dark field image of yeast cells with Ag NPs (× 100 objective), scale bars are 1 µm, **(c)** AFM images of an yeast cell surface. Ag NP dimers adsorbed are circled and added in lower panels. Reproduced from Ref. [29].
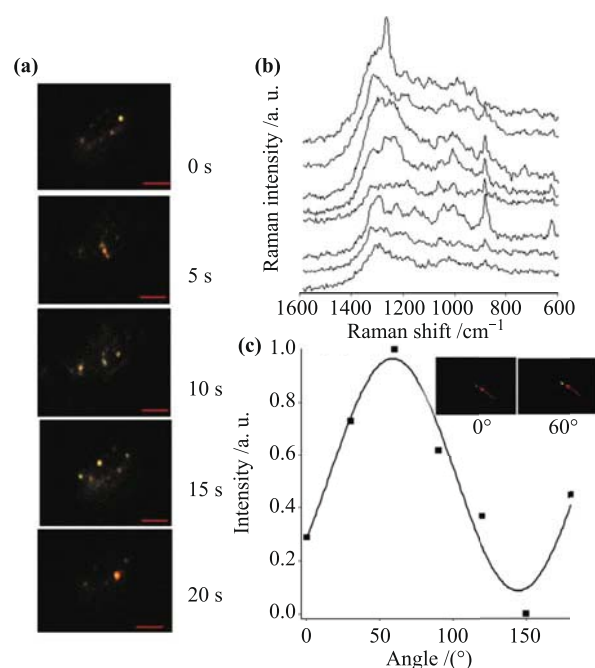

Fig. 4 Temporal and polarization dependence of SERS: **(a)** Blinking of SERS spots from Ag NP aggregates on a single yeast cell wall (×60 objective), scale bars are 1 µm, **(b)** temporal changes in SERS spectra from a single Ag NP aggregate on a yeast cell wall recorded at 2 minute intervals, and **(c)** polarization dependence of SERS intensity; inset is SERS spots used for the polarization dependence measurement. Reproduced from Ref. [29].

few molecules detections; thus, these SERS spectra may be from single or few biomolecules on the yeast cell wall. Polarization dependence of SERS signals in Fig. 4(c) from single Ag NP aggregates indicates that the signals are from amplified EM field at nanometric gaps between Ag NPs [16].

We tried to identify the molecular species generating SERS signals on living single yeast cell wall by comparing Raman and SERS spectra of mannan, glucan and chitin, which are the main components of yeast cell wall. We found that the SERS spectra of mannan ex-

tracted from *Saccharomyces cerevisiae* strain are similar to the SERS spectra; however, Raman spectra of mannan, which do not have affinity to Ag NPs, largely different from SERS spectra. Finally we attributed the SERS spectra to mannoproteins, which have affinity to Ag NPs, included in mannan [29–31]. These observations demonstrate a site specific method for detecting cell wall proteins and will be useful to understand biochemical conditions in yeast cell walls. Not only the spot-by-spot SERS detections in Fig. 5(a), scanning imaging of the cell wall of living single yeast cell with weak laser excitation ($\sim$15 W/cm^2) has been also successfully carried out as shown in Fig. 5(b) [30].

Nevertheless the successful measurement in SERS on yeast cell wall, there is a certain limitation of SERS measurement using Ag NPs to other type of cells. The limitation is an affinity of molecules to Ag surfaces because the affinity is a primary requirement for adsorption of Ag NPs on cell surfaces to realize large Raman enhancement. This requirement limits ability of SERS to various fields of biosensing. We introduce here a photo-reduction strategy to resolve the limitation by directly preparing Ag NPs on cell surfaces [32, 33]. *Helicobacter pylori* (*H. pylori*), which is one of the most widely known pathogenic bacteria, was our second choice for SERS biosensing for cells. We confirmed that *H. pylori* does not show affinity for externally added Ag NPs. Thus, we achieved to directly photo-reduce Ag NPs on the surface of *H. pylori* by loosely focusing a green laser ($\sim$260 W/cm^2) in a sus-

pension of bacteria with Ag nitrate and citric acid. Then aggregates of bacteria began to show detectable SERS signals within 10 second from Ag NP aggregates which were photo-reduced on their surfaces under continuous irradiation of the green laser. The SERS spectra contain enhanced amid bands. Using Raman cross-section of an amide band (4.46×10^{-29} cm^2) and that of the enhanced amide band (1.77×10^{-18} cm^2), the SERS enhancement factor is estimated to be $\sim$10^{11} [32]. EM enhancement contribution to SERS enhancement factors is usually around 10^8; thus, the chemical enhancement contribution may be $<\sim$10^3 in the present SERS system [32]. Figure 6 summarizes the strategy using photo-reduced Ag NPs for SERS detections of cell surfaces which do not have affinity to Ag NPs. The present photo-reduction strategy of SERS has been applied to single cell detection by combining NIR trapping laser and photo-reduction green laser. We have succeeded to selectively measure SERS spectra of single *E. coli* cell surfaces, which are our third choice as cell target [33]. The comparison with previous collective SERS measurements suggests that the origin of SERS spectra is attributed to flavin adenine dinucleotide (FAD) [33].

3.4 Applications of SERS to biomarker sensing

Another attractive bio-application in SERS is label-free sensing of biomarkers. SERS is a valuable tool for characterizing biomolecules such as heme [7, 102–108], DNA
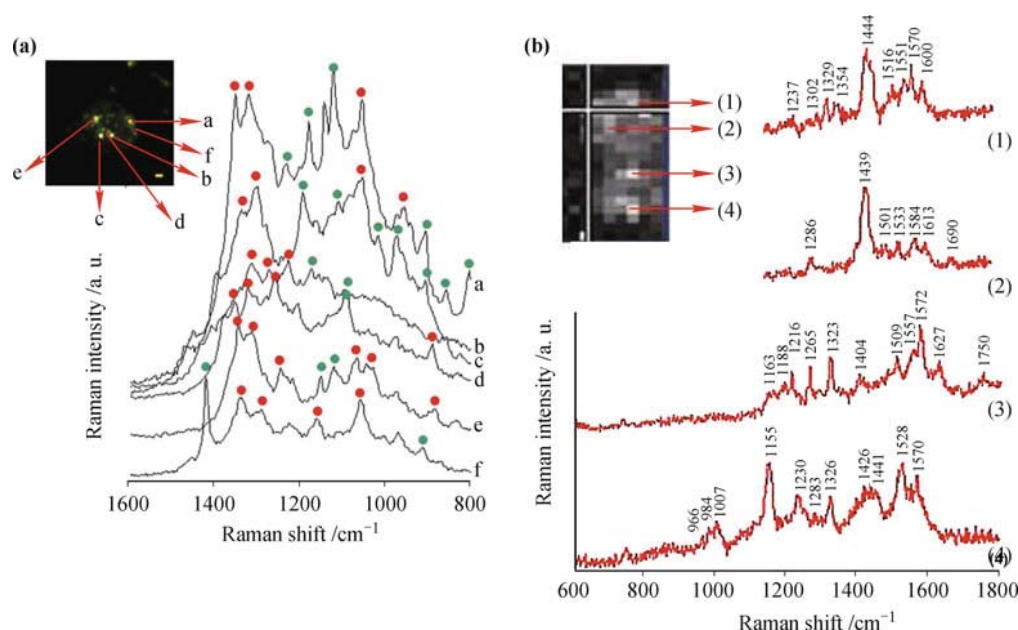

Fig. 5 SERS image and SERS spectra: **(a)** Ag NP aggregate-by-aggregate variations in SERS spectra a single yeast cell wall, the spectra "a" to "f" were collected from Ag NP aggregates "a" to "f" in the image, **(b)** Ag NP aggregate-by-aggregate variations in SERS spectra a single yeast cell wall, the spectra "a" to "f" were collected from Ag NP aggregates "a" to "f" in the image, the spectra (1) to (4) were collected from positions (1) to (4) in the image, ($\times$100 objective, scale bar is 1 μm. Reproduced from Refs. [29, 30].
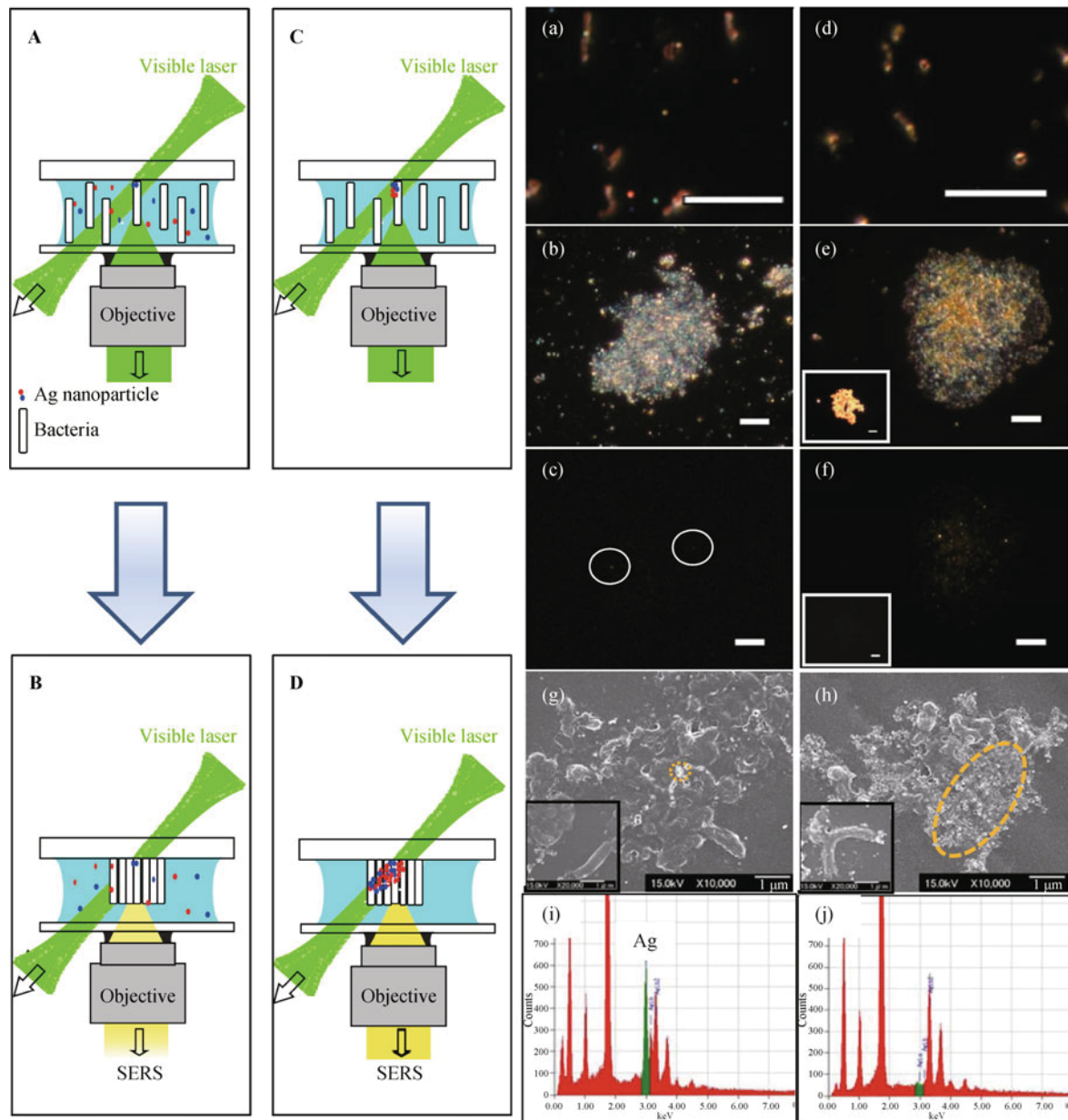
Fig. 6 Strategy of SERS measurement using photo-reduced Ag NPs: **(A)** schematics of an experimental procedure for SERS measurements of a single bacterium using colloidal Ag NPs, **(B)** that for SERS measurements of a bacterial aggregate using colloidal Ag NPs, **(C)** that for SERS measurements of a single bacterium using photo-reduction of silver nitrate, and **(D)** that for SERS measurements of a bacterial aggregate using photo-reduction of silver nitrate. (a) A dark field image of isolated single bacteria in Ag NP colloidal solution, (b) that of a bacterial aggregate in Ag colloidal solution, (c) a SERS image of a bacterial aggregate in Ag NP colloidal solution, (d) a dark field image of isolated single bacteria in Ag nitrate solution, (e) that of a bacterial aggregate in Ag nitrate solution, (f) a SERS image of a bacterial aggregate in Ag nitrate solution. Inset of (e) and (f): A dark field image and a SERS image of a large Ag NP aggregate with citric acid. Scales of (a) to (f) are all 10 μm. (g) A SEM image of a bacterial aggregate with Ag NPs and (h) that of a bacterial aggregate with Ag nitrate after laser irradiation. Inset of (g) and (h): Enlarged image of single bacteria. (i) and (j): EDS spectra inside and outside an orange circle with dashed line on bacterial aggregates in (g, h), respectively. Reproduced from Ref. [32].

[109], and cytochromes [110, 111] because of its ultimate sensitivity by 10–14 orders of magnitude compared with normal Raman signal. SERS spectroscopy fundamentally enables us label-free analysis of molecules. Thus, we can sensitively and selectively detect and identify biomolecules due to the distinct vibrational spectrum of each molecule.

For label-free sensing of biomarkers, we report on selective detection of hemoglobin A1c (HbA1c) [34], which is a marker for glycemic control in diabetic patients,

using SERS spectroscopy. SERS spectra of Ag NP aggregates adsorbed by hemoglobin A (HbA) and HbA1c were measured under 532 nm excitation. The adsorption is carried out by incubating Ag NPs to HbA molecules for 3 h at room temperature. Figures 7(a) and (b) are SERS spectra of HbA and HbA1c, respectively. As shown in Fig. 7(c), remarkable spectral differences between SERS of HbA and that of HbA1c were observed. A SERS spectrum of HbA shows bands at 1403 and 1652 cm^{-1} as indicated in Fig. 7(a). In the case of SERS of HbA1c, we found a predominant band at 827±50 cm^{-1} in addition to the vibrations of porphyrin rings as indicated in Fig. 7(c). Thus, the band around 827 cm^{-1} can be a key for distinguishing HbA1c from HbA. However the band is not reported until now; thus, the band assignment is needed. The major difference between HbA and HbA1c is the presence of a covalently attached glucose moiety in the former. We compared the Raman and SERS spectra of pure glucose. However, the glucose solution neither caused the aggregation of Ag NPs nor produced the
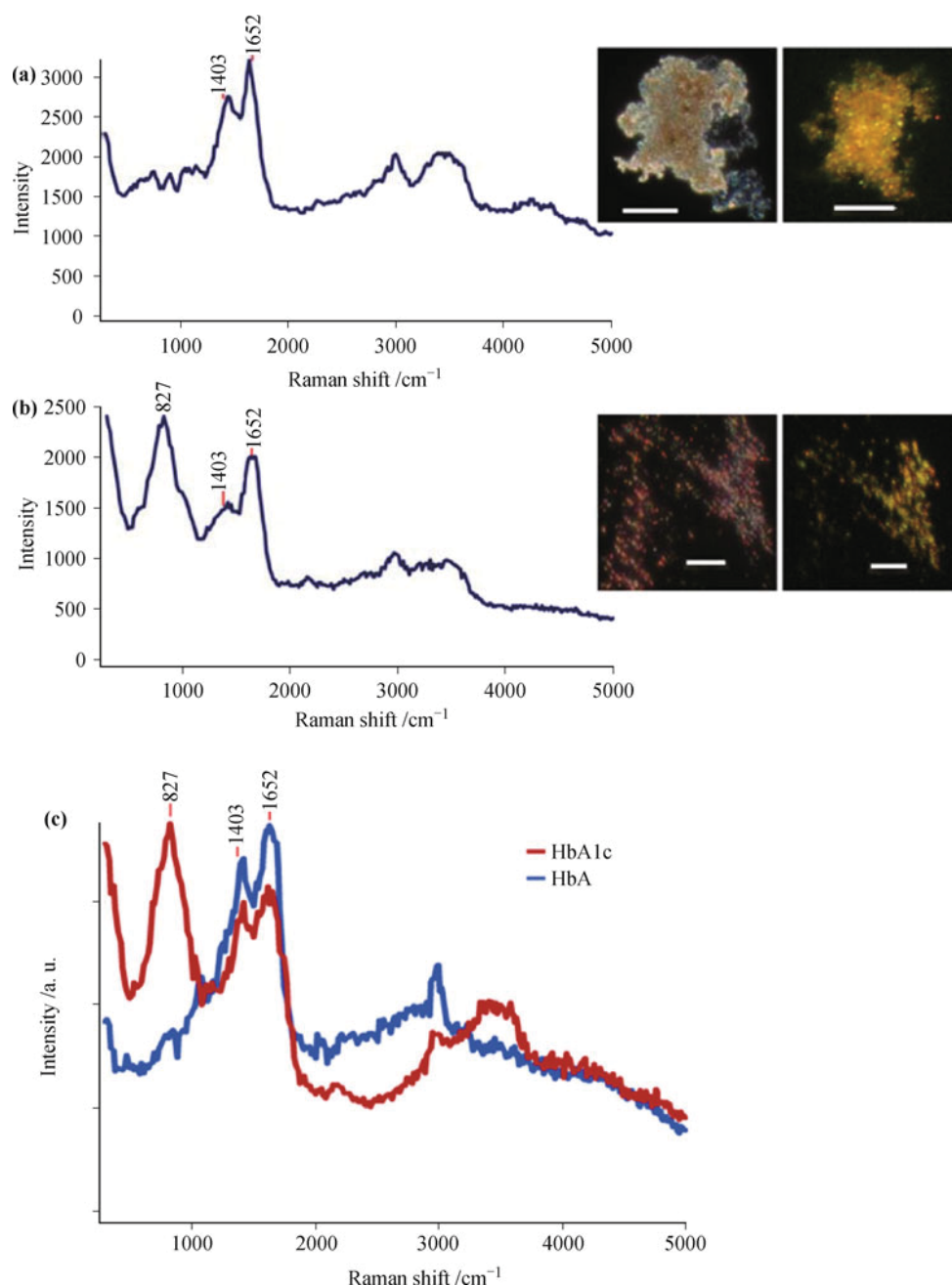
Fig. 7 SERS spectra of HbA and HbA1c. HbA and HbA1c were incubated with Lee–Meisel Ag NP colloidal solution and their SERS spectra measured with excitation at 532 nm, power 2 W/cm^2 on the sample: **(a)** SERS spectrum, SERS image, and dark field image (×60 objective) of HbA (1.5×10^{-6} M), **(b)** SERS spectrum, SERS image, and dark field image (×60 objective) of HBA1c (1.5×10^{-6} M), **(c)** SERS spectrum of HbA and that of HbA1c. Reproduced from Ref. [34].

40

Yuko S. Yamamoto, et al., Front. Phys., 2014, 9(1)

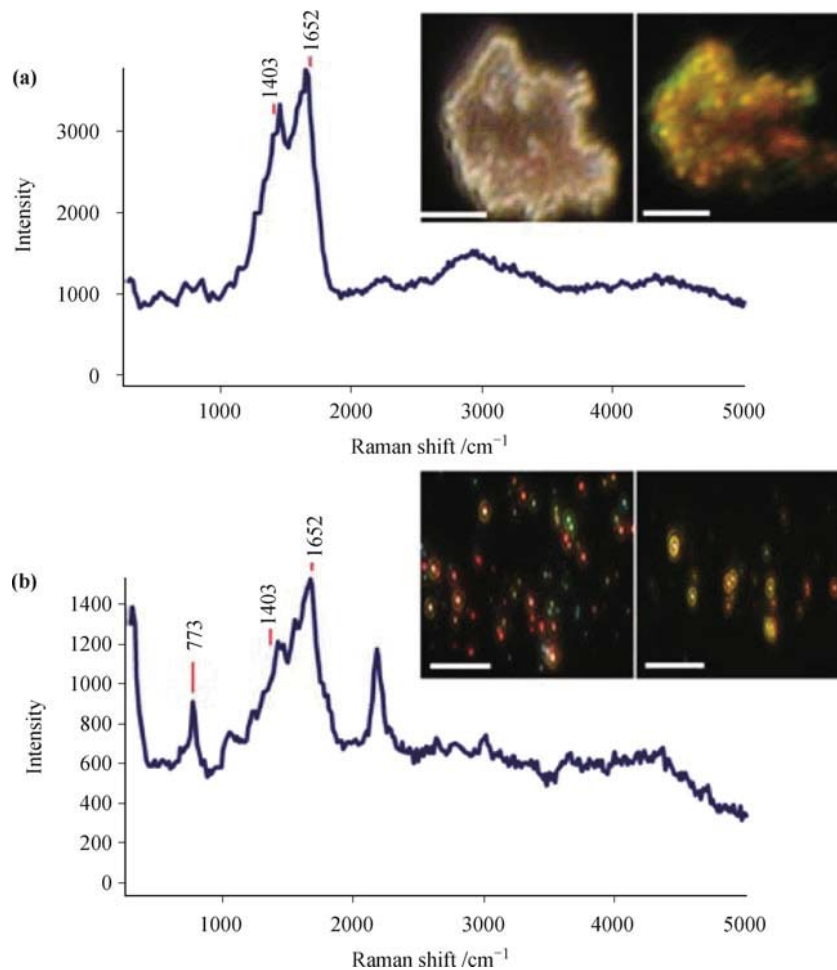**Fig. 8** SERS of HbA incubated with glucose: HbA (1.5×10^{-5} M) (500 μL) was mixed with 8 mg glucose and kept at room temperature for one week. After one week the HbA glucose mixture was incubated with Ag NP colloidal solution. The supernatant and sediment were collected and SERS spectra was measured for both supernatant and sediment: **(a)** SERS spectrum, dark field image, and SERS image (×60 objective) of sediment, and **(b)** SERS spectrum, dark field image, and SERS image (×60 objective) of supernatant. Scale bars are 10 μm. Reproduced from Ref. [34].

characteristic band, not indicating that the contribution of free glucose to the band around 827 cm^{-1}. We tentatively considered that structural changes in HbA associated with the binding of glucose moiety generate the band around 827 cm^{-1}. The appearance of SERS band around 827 cm^{-1} for HbA1c suggests that the glucosyl residue attached to HbA contributed to the characteristic band.

To further investigate the origin of the key band, we non-enzymatically reacted HbA with glucose and analyzed the SERS spectrum of the reaction mixture. 1 mg /ml solution of HbA with 8 mg glucose at room temperature for a week. An aliquot of this mixture (1.5×10^{-6} M HbA) was incubated with colloidal solution of Ag NPs and the supernatant and sediment were separated and subjected to SERS spectroscopy. We observed characteristics spectral band around 773 cm^{-1}, whose position is within the energy fluctuation of the key band around 827

cm^{-1}, in case of supernatant [Fig. 8 (b)], compared to sediment [Fig. 8 (a)]. SERS spectra of supernatant and those of sediment are similar to SERS spectra of HbA1c and those of HbA respectively. The appearance of band around 773 cm^{-1} in the supernatant indicates the formation of glycosylated HbA, that is HbA1c, due to the non-enzymatic reaction of glucose with HbA. Finally we conclude that the appearance of the characteristic band in HbA1c is induced by the glucosyl residue attached to the HbA.

In this study we reported selective detection of HbA1c from HbA. The spectrally distinct SERS band at position in 827 ± 50 cm^{-1} was the origin of this selective detection. The occurrence of this band is attributed to the glucosyl moiety attached to the HbA1c. The assignment of the band was confirmed by non-enzymatically produced HbA1c with glucose. However, we note the lack of quantitative analysis of HbA1c in the study. The quantitative

analysis can be resolved by using standard SERS substrates developed in other groups [112–114].

3.5 Summary

In this section, we have reviewed our recent exploration in SERS for biosensing as well as the advantages of SERS spectroscopy for label-free detection of biomolecules. We have introduced SERS spectroscopy of yeast cell surfaces to characterize cell surface proteins [29–31]. Observations of SERS blinking made it clear that SERS signals were coming from single or few biomolecules, presumably mannoproteins, which are rich in yeast cell surfaces [29–31]. We also successfully detected SERS spectra from cell surfaces of *Helicobacter pylori* and *E. coli,* which do not have affinity to Ag NPs, with introducing photo-reduction strategy [32, 33]. Furthermore, Hemoglobin A1c, which is a biomarker in diabetes, has explored by SERS. We succeeded selective detection of HbA1c from HbA and showed a potential to separate SERS signal of HbA1c from its HbA in a mixture [34]. Our findings may open up research for the development of SERS-based sensors for HbA1c as diagnostic tool in the diagnosis of diabetes.

4 Conclusion

In this mini-review, we have summarized our recent studies on experimental investigations in SERS to quantitatively validate the EM mechanism. In these studies, SERS spectra, plasmon resonance spectra, and shapes of Ag NP dimers are directly compared in the framework of EM mechanism, resulting in quantitative evaluation of SERS enhancement and SERS blinking mechanism. The advantages of SERS spectroscopy for label-free detection of biomolecules have been described to emphasize the potential of SERS for biosensing. As demonstration of the SERS biosensing, we also introduced our SERS studies. Four types of biological targets; yeast, *helicobacter pylori, E. coli*, and hemoglobin A1c have been investigated using SERS as potential targets incorporated to future progress in SERS application. We are now improving new SERS spectroscopic instrumentation to resolve the intrinsic spatial inhomogeneity of SERS spectra, which deteriorate quality of SERS biosensing, by using cost effective hyper-spectral imaging systems [115].

References

1. M. Fleischman, P. J. Hendra, and A. J. McQuillan, Raman spectra of pyridine adsorbed at a silver electrode, *Chem. Phys. Lett.*, 1974, 26(2): 123

2. M. G. Albrecht and J. A. Creighton, Anomalously intense Raman spectra of pyridine at a silver electrode, *J. Am. Chem. Soc.*, 1977, 99(15): 5215

3. D. L. Jeanmaire and R. P. V. Duyne, Surface raman spectroelectrochemistry, *J. Electroanal. Chem.*, 1977, 84(1): 1

4. K. Kneipp, M. Moskovits, and H. Kneipp, Surface-Enhanced Raman Scattering, Heidelberg: Springer, 2006

5. K. Kneipp, Y. Wang, H. Kneipp, L. Perelman, I. Itzkan, R. R. Dasari, and M. Feld, Single molecule detection using surface-enhanced Raman scattering (SERS), *Phys. Rev. Lett.*, 1997, 78(9): 1667

6. S. Nie and S. R. Emory, Probing single molecules and single nanoparticles by surface-enhanced Raman scattering, *Science*, 1997, 275(5303): 1102

7. H. Xu, E. Bjerneld, M. Käll, and L. Borjesson, Spectroscopy of single hemoglobin molecules by surface enhanced Raman scattering, *Phys. Rev. Lett.*, 1999, 83(21): 4357

8. A. Micheals, M. Nirmal, and L. Brus, Surface enhanced Raman spectroscopy of individual rhodamine 6G molecules on large Ag nanocrystals, *J. Am. Chem. Soc.*, 1999, 121(43): 9932

9. J. A. Dieringer, K. A. Lettan, Scheidt, and R. P. Van Duyne, A frequency domain existence proof of single-molecule surface-enhanced Raman spectroscopy, *J. Am. Chem. Soc.*, 2007, 129(51): 16249

10. Y. C. Cao, R. Jin, and C. A. Mirkin, Nanoparticles with Raman spectroscopic fingerprints for DNA and RNA detection., *Science*, 2002, 297(5586): 1536

11. X. Qian, X. H. Peng, D. O. Ansari, Q. Yin-Goen, G. Z. Chen, D. M. Shin, L. Yang, A. N. Young, M. D. Wang, and S. M. Nie, In vivo tumor targeting and spectroscopic detection with surface-enhanced Raman nanoparticle tags, *Nat. Biotechnol.*, 2008, 26(1): 83

12. J. N. Anker, W. P. Hall, O. Lyandres, N. C. Shah, J. Zhao, and R. P. Van Duyne, Biosensing with plasmonic nanosensors, *Nat. Mater.*, 2008, 7(6): 442

13. J. F. Li, Y. F. Huang, Y. Ding, Z. L. Yang, S. B. Li, X. S. Zhou, F. R. Fan, W. Zhang, Z. Y. Zhou, D. Y. Wu, B. Ren, Z. L. Wang, and Z. Q. Tian, Shell-isolated nanoparticle-enhanced Raman spectroscopy, *Nature*, 2010, 464: 392

14. H. Xu, J. Aizpurua, M. Käll, and P. Apell, Electromagnetic contributions to single-molecule sensitivity in surface-enhanced raman scattering, *Phys. Rev. E*, 2000, 62(3): 4318

15. M. Inoue, and K. Ohtaka, Surface enhanced Raman scattering by metal spheres (I): Cluster effect, *J. Phys. Soc. Jpn.*, 1983, 52(11): 3853

16. K. Yoshida, T. Itoh, H. Tamaru, V. Biju, M. Ishikawa, and Y. Ozaki, Quantitative evaluation of electromagnetic en-

hancement in surface-enhanced resonance Raman scattering from plasmonic properties and morphologies of individual Ag nanostructures, *Phys. Rev. B*, 2010, 81(11): 115406

17. D. Wang and M. Kerker, Enhanced Raman scattering by molecules adsorbed at the surface of colloidal spheroids, *Phys. Rev. B*, 1981, 24(4): 1777

18. M. Moskovits, Surface-enhanced spectroscopy, *Rev. Mod. Phys.*, 1985, 57(3): 783

19. B. Pettinger, Light scattering by adsorbates at Ag particles: Quantum-mechanical approach for energy transfer induced interfacial optical processes involving surface plasmons, multipoles, and electron-hole pairs, *J. Chem. Phys.*, 1986, 85(12): 7442

20. H. Xu, X. H. Wang, M. P. Persson, H. Q. Xu, M. Käll, and P. Johansson, Unified treatment of fluorescence and raman scattering processes near metal surfaces, *Phys. Rev. Lett.*, 2004, 93(24): 243002

21. J. R. Lombardi, R. L. Birke, T. Lu, and J. Xu, Charge-transfer theory of surface enhanced Raman spectroscopy: Herzberg–Teller contributions, *J. Chem. Phys.*, 1986, 84(8): 4174

22. A. Otto, I. Mrozek, H. Grabhorn, and W. Akemann, Surface-enhanced Raman scattering, *J. Phys.: Condens. Matter*, 1992, 4(5): 1143

23. A. Campion and P. Kambhampati, Surface-enhanced Raman scattering, *Chem. Soc. Rev.*, 1998, 27(4): 241

24. R. L. Birke, V. Znamenskiy, and J. R. Lombardi, A charge-transfer surface enhanced Raman scattering model from time-dependent density functional theory calculations on a Ag10-pyridine complex, *J. Chem. Phys.*, 2010, 132(21): 214707

25. D. Y. Wu, J. F. Li, B. Ren, and Z. Q. Tian, Electrochemicalsurface-enhanced Raman spectroscopy of nanostructures, *Chem. Soc. Rev.*, 2008, 37(5): 1025

26. K. Imura, H. Okamoto, M. K. Hossain, and M. Kitajima, Visualization of localized intense optical fields in single gold-nanoparticle assemblies and ultrasensitive Raman active sites, *Nano Lett.*, 2006, 6(10): 2173

27. E. Le Ru and P. Etchegoin, Rigorous justification of the $|E|^4$ enhancement factor in surface enhanced Raman spectroscopy, *Chem. Phys. Lett.*, 2006, 423(1–3): 63

28. S. A. Meyer, E. C. Le Ru, and P. G. Etchegoin, Quantifying resonant Raman cross sections with SERS, *J. Phys. Chem. A*, 2010, 114(17): 5515

29. A. Sujith, T. Itoh, H. Abe, A. A. Anas, K. Yoshida, V. Biju, and M. Ishikawa, Surface enhanced Raman scattering analyses of individual silver nanoaggregates on living single yeast cell wall, *Appl. Phys. Lett.*, 2008, 92(10): 103901

30. A. Sujith, T. Itoh, H. Abe, K. Yoshida, M. S. Kiran, V. Biju, and M. Ishikawa, Imaging the cell wall of living single yeast cells using surface-enhanced Raman spectroscopy, *Anal. Bioanal. Chem.*, 2009, 394(7): 1803

31. M. S. Kiran, H. Abe, Y. Fujita, K. Tomimoto, V. Biju, M. Ishikawa, Y. Ozaki, and T. Itoh, Inhibition assay of

yeast cell walls by plasmon resonance Rayleigh scattering and surface-enhanced Raman scattering imaging, *Langmuir*, 2012, 28(14): 8952

32. H. Kudo, T. Itoh, T. Kashiwagi, M. Ishikawa, H. Takeuchi, and H. Ukeda, Surface enhanced Raman scattering spectroscopy of Ag nanoparticle aggregates directly photo-reduced on pathogenic bacterium (Helicobacter pylori), *J. Photochem. Photobiol. Chem.*, 2011, 221(2–3): 181

33. Y. Kitahama, T. Itoh, T. Ishido, K. Hirano, and M. Ishikawa, Surface-enhanced Raman scattering from photoreduced Ag nanoaggregates on an optically trapped single bacterium, *Bull. Chem. Soc. Jpn.*, 2011, 84(9): 976978

34. M. S. Kiran, T. Itoh, K. Yoshida, N. Kawashima, V. Biju, and M. Ishikawa, Selective detection of HbA1c using surface enhanced resonance Raman spectroscopy, *Anal. Chem.*, 2010, 82(4): 1342

35. K. Yoshida, T. Itoh, V. Biju, M. Ishikawa, and Y. Ozaki, Experimental evaluation of the twofold electromagnetic enhancement theory of surface-enhanced resonance Raman scattering, *Phys. Rev. B*, 2009, 79(8): 085419

36. T. Itoh, K. Yoshida, V. Biju, Y. Kikkawa, M. Ishikawa, and Y. Ozaki, Second enhancement in surface-enhanced resonance Raman scattering revealed by an analysis of anti-Stokes and Stokes Raman spectra, *Phys. Rev. B*, 2007, 76(8): 085405

37. T. Itoh, K. Yoshida, H. Tamaru, V. Biju, and M. Ishikawa, Experimental demonstration of the electromagnetic mechanism underlying surface enhanced Raman scattering using single nanoparticle spectroscopy, *J. Photochem. Photobiol. Chem.*, 2011, 219(2–3): 167

38. T. Itoh, M. Iga, H. Tamaru, K. Yoshida, V. Biju, and M. Ishikawa, Quantitative evaluation of blinking in surface enhanced resonance Raman scattering and fluorescence by electromagnetic mechanism, *J. Chem. Phys.*, 2012, 136(2): 024703

39. S. Habuchi, M. Cotlet, R. Gronheid, G. Dirix, J. Michiels, J. Vanderleyden, F. C. De Schryver, and J. Hofkens, Single-molecule surface enhanced resonance Raman spectroscopy of the enhanced green fluorescent protein, *J. Am. Chem. Soc.*, 2003, 125(28): 8446

40. J. Zhao, L. Jensen, J. Sung, S. Zou, G. C. Schatz, and R. P. Duyne, Interaction of plasmon and molecular resonances for rhodamine 6G adsorbed on silver nanoparticles, *J. Am. Chem. Soc.*, 2007, 129(24): 7647

41. R. M. Dickson, A. B. Cubitt, R. Y. Tsien, and W. E. Moerner, On/off blinking and switching behaviour of single molecules of green fluorescent protein, *Nature*, 1997, 388(6640): 355

42. J. Yu, D. Hu, and P. F. Barbara, Unmasking electronic energy transfer of conjugated polymers by suppression of O_2 quenching, *Science*, 2000, 289(5483): 1327

43. K. A. Bosnick, J. Jiang, and L. E. Brus, Fluctuations and local symmetry in single-molecule rhodamine 6G Raman scat-

Frontiers of Physics

Yuko S. Yamamoto, et al., Front. Phys., 2014, 9(1)

43

tering on silver nanocrystal aggregates, *J. Phys. Chem. B*, 2002, 106(33): 8096

44. S. R. Emory, R. A. Jensen, T. Wenda, M. Y. Han, and S. M. Nie, Re-examining the origins of spectral blinking in single-molecule and single-nanoparticle SERS, *Faraday Discuss.*, 2006, 132: 249

45. Z. Wang and L. J. Rothberg, Origins of blinking in single-molecule Raman spectroscopy, *J. Phys. Chem. B*, 2005, 109(8): 3387

46. A. Weiss and G. Haran, Time-dependent single-molecule Raman scattering as a probe of surface dynamics, *J. Phys. Chem. B*, 2001, 105(49): 12348

47. M. Moskovits, L. L. Tay, J. Yang, and T. Haslett, SERS and the single molecule, *Top. Appl. Phys.*, 2002, 82: 215

48. P. Lee and D. Misel, Adsorption and surface-enhanced Raman of dyes on silver and gold sols, *J. Phys. Chem.*, 1982, 86(17): 3391

49. T. Itoh, Y. Kikkawa, K. Yoshida, K. Hashimoto, V. Biju, M. Ishikawa, and Y. Ozaki, Correlated measurements of plasmon resonance Rayleigh scattering and surface-enhanced resonance Raman scattering using a dark-field microspectroscopic system, *J. Photochem. Photobiol. Chem.*, 2006, 2183(3): 322

50. A. Otto, Theory of first layer and single molecule surface enhanced Raman scattering (SERS), *Phys. Status Solidi*, 2001, 188(4): 1455

51. J. M. Reyes-Goddard, H. Barr, and N. Stone, Photodiagnosis using Raman and surface enhanced Raman scattering of bodily fluids, *Photodiagn. Photodyn. Ther.*, 2005, 2(3): 223

52. S. Farquharson, A. D. Gift, C. Shende, P. Maksymiuk, F. E. Inscore, and J. Murran, Detection of 5-fluorouracil in saliva using surface-enhanced Raman spectroscopy, *Vib. Spectrosc.*, 2005, 38(1–2): 79

53. G. Breuzarda, O. Piota, J. F. Angibousta, M. Manfaita, L. Candeilb, M. Del Riob, and J. M. Millota, Changes in adsorption and permeability of mitoxantrone on plasma membrane of BCRP/MXR resistant cells, *Biochem. Biophys. Res. Commun.*, 2005, 329(1): 64

54. V. P. Drachev, M. D. Thoreson, V. Nashine, E. N. Khaliullin, D. Ben-Amotz, V. J. Davisson, and V. M. Shalaev, Adaptive silver films for surface-enhanced Raman spectroscopy of biomolecules, *J. Raman Spectrosc.*, 2005, 36: 648

55. R. M. Jarvis, A. Brooker, and R. Goodacre, Surface-enhanced Raman scattering for the rapid discrimination of bacteria, *Faraday Discuss.*, 2006, 132: 281

56. F. Yan, and T. Vo-Dinh, Surface-enhanced Raman scattering detection of chemical and biological agents using a portable Raman integrated tunable sensor, *Sens. Actuators B Chem.*, 2007, 121(1): 61

57. T. M. Cotton, S. G. Schultz, and R. P. Van Duyne, Surface-enhanced resonance Raman scattering from cytochrome c and myoglobin adsorbed on a silver electrode, *J. Am. Chem. Soc.*, 1980, 102(27): 7960

58. H. Morjani, J. F. Riou, I. Nabiev, F. Lavelle, and M. M. Manfait, Molecular and cellular interactions between intoplicine, DNA, and topoisomerase II studied by surface-enhanced Raman scattering spectroscopy, *Cancer Res.*, 1993, 53(20): 4784

59. M. Manfait, H. Morjani, and I. Nabiev, Molecular events on simple living cancer cells as studied by spectrofluorometry and micro-SERS Raman spectroscopy, *J. Cell. Pharmacol.*, 1992, 3: 120

60. I. R. Nabiev, H. Morjani, and M. Manfait, Selective analysis of antitumor drug interaction with living cancer cells as probed by surface-enhanced Raman spectroscopy, *Eur. Biophys. J.*, 1991, 19(6): 311

61. K. K. Sandhu, C. M. McIntosh, J. M. Simard, S. W. Smith, and V. M. Rotello, Gold nanoparticle-mediated transfection of mammalian cells, *Bioconjug. Chem.*, 2002, 13(1): 3

62. G. Han, C. C. You, B. J. Kim, R. S. Turingan, N. S. Forbes, C. T. Martin, and V. M. Rotello, Light-regulated release of DNA and its delivery to nuclei by means of photolabile gold nanoparticles, *Angew. Chem. Int. Ed. Engl.*, 2006, 45(19): 3165

63. R. M. Jarvis and R. Goodacre, Discrimination of bacteria using surface-enhanced Raman spectroscopy, *Anal. Chem.*, 2004, 76(1): 40

64. J. Kneipp, H. Kneipp, M. McLaughlin, D. Brown, and K. Kneipp, In vivo molecular probing of cellular compartments with gold nanoparticles and nanoaggregates, *Nano Lett.*, 2006, 6(10): 2225

65. L. Zeiri, B. V. Bronk, Y. Shabtai, J. Eichler, and S. Efrima, Surface-enhanced Raman spectroscopy as a tool for probing specific biochemical components in bacteria, *Appl. Spectrosc.*, 2004, 58(1): 33

66. C. Eliasson, A. Lorén, J. Engelbrektsson, M. Josefson, J. Abrahamsson, and K. Abrahamsson, Surface-enhanced Raman scattering imaging of single living lymphocytes with multivariate evaluation, *Spectrochim. Acta A: Mol. Biomol. Spectrosc.*, 2005, 61(4): 755

67. K. Kneipp, H. Kneipp, I. Itzkan, R. R. Dasari, and M. S. Feld, Ultrasensitive chemical analysis by Raman spectroscopy, *Chem. Rev.*, 1999, 99(10): 2957

68. Y. C. Cao, R. Jin, and C. A. Mirkin, Nanoparticles with Raman spectroscopic fingerprints for DNA and RNA detection, *Science*, 2002, 297(5586): 1536

69. K. Kneipp, H. Kneipp, and J. Kneipp, Surface-enhanced Raman scattering in local optical fields of silver and gold nanoaggregates-from single-molecule Raman spectroscopy to ultrasensitive probing in live cells, *Acc. Chem. Res.*, 2006, 39(7): 443

70. W. R. Premasiri, D. T. Moir, M. S. Klempner, N. Krieger, G. Jones, and L. D. Ziegler, Characterization of the surface enhanced raman scattering (SERS) of bacteria, *J. Phys. Chem. B*, 2005, 109(1): 312

71. J. Rejman, V. Oberle, I. S. Zuhorn, and D. Hoekstra, Size-dependent internalization of particles via the pathways of

Frontiers of Physics

clathrin- and caveolae-mediated endocytosis, *Biochem. J.*, 2004, 377: 159

72. W. J. Arlein, J. D. Shearer, and M. D. Caldwell, Continuity between wound macrophage and fibroblast phenotype: analysis of wound fibroblast phagocytosis, *Am. J. Physiol.*, 1998, 275: R1041

73. A. G. Tkachenko, H. Xie, Y. L. Liu, D. Coleman, J. Ryan, W. R. Glomm, M. K. Shipton, S. Franzen, and D. L. Feldheim, Cellular trajectories of peptide-modified gold particle complexes: comparison of nuclear localization signals and peptide transduction domains, *Bioconjug. Chem.*, 2004, 15(3): 482

74. P. R. Carey, Resonance Raman labels and Raman labels, *J. Raman Spectrosc.*, 1998, 29(10–11): 861

75. K. Nithipatikom, M. J. McCoy, S. R. Hawi, K. Nakamoto, F. Adar, and W. B. Campbell, Characterization and application of Raman labels for confocal Raman microspectroscopic detection of cellular proteins in single cells, *Anal. Biochem.*, 2003, 322(2): 198

76. C. E. Talley, T. R. Huser, C. W. Hollars, L. Jusinski, T. Laurence, and S. M. Lane, Nanoparticle Based Surface-Enhanced Raman Spectroscopy, UCRL-PROC-208863, NATO Advanced Study Institute: Biophotonics Ottawa, Canada, 2005

77. C. E. Talley, L. Jusinski, C. W. Hollars, S. M. Lane, and T. Huser, Intracellular pH sensors based on surface-enhanced Raman scattering, *Anal. Chem.*, 2004, 76(23): 7064

78. B. Alberts, and D. Bray, D, J. Lewis, M. Raff, K. Roberts, and J. D. Watson, Molecular Biology of the Cell, New York: Garland Publishing, 1994

79. M. Fukasawa, F. Sekine, M. Miura, M. Nishijima, and K. Hanada, Involvement of heparan sulfate proteoglycans in the binding step for phagocytosis of latex beads by Chinese hamster ovary cells, *Exp. Cell Res.*, 1997, 230(1): 154

80. R. J. Dijkstra, W. J. J. M. Scheenen, N. Dam, E. W. Roubos, and J. J. ter Meulen, Monitoring neurotransmitter release using surface-enhanced Raman spectroscopy, *J. Neurosci. Methods*, 2007, 159(1): 43

81. R. H. Chow, L. von Rüden, and E. Neher, Delay in vesicle fusion revealed by electrochemical monitoring of single secretory events in adrenal chromaffin cells, *Nature*, 1992, 356(6364): 60

82. T. Vo-Dinh, F. Yan, and M.B. Wabuyele, Surface-enhanced Raman scattering for medicaldiagnostics and biological imaging, *J. Raman Spectrosc.,* 2005, 36: 640

83. T. Vo-Dinh, P. Kasili, and M. Wabuyele, Nanoprobes and nanobiosensors for monitoring and imaging individual living cells, *Nanomed.: Nanotechnol. Biol. Med.*, 2006, 2(1): 22

84. S. Lee, S. Kim, J. Choo, S. Y. Shin, Y. H. Lee, H. Y. Choi, S. Ha, K. Kang, and C. H. Oh, Biological imaging of HEK293 cells expressing PLCgamma1 using surface-enhanced Raman microscopy, *Anal. Chem.*, 2007, 79(3): 916

85. G. R. Souza, D. R. Christianson, F. I. Staquicini, M. G. Ozawa, E. Y. Snyder, R. L. Sidman, J. H. Miller, W. Arap, and R. Pasqualini, Networks of gold nanoparticles and bacteriophage as biological sensors and cell-targeting agents, *Proc. Natl. Acad. Sci. USA*, 2006, 103(5): 1215

86. Q. Hu, L. L. Tay, M. Noestheden, and J. P. Pezacki, Mammalian cell surface imaging with nitrile-functionalized nanoprobes: biophysical characterization of aggregation and polarization anisotropy in SERS imaging, *J. Am. Chem. Soc.*, 2007, 129(1): 14

87. G. U. Puppel, F. F. M. De Mul, C. Otto, J. Greve, M. Robert-Nicoud, D. J. Arndt-Jovin, and T. M. Jovin, Studying single living cells and chromosomes by confocal Raman microspectroscopy, *Nature*, 1990, 347: 301

88. W. L. Peticolas, T. W. Patapoff, G. A. Thomas, J. Postlewait, and J. W. Powell, Laser Raman microscopy of chromosomes in living eukaryotic cells: DNA polymorphisim in vivo, *J. Raman Spectrosc.*, 1996, 27: 571

89. B. B. Chomel, Control and prevention of emerging zoonoses, *J. Vet. Med. Educ.*, 2003, 30(2): 145

90. R. M. Jarvis and R. Goodacre, Discrimination of bacteria using surface-enhanced Raman spectroscopy, *Anal. Chem.*, 2004, 76(1): 40

91. S. E. J. Bell, J. N. Mackle, and N. M. S. Sirimuthu, Quantitative surface-enhanced Raman spectroscopy of dipicolinic acid – towards rapid anthrax endospore detection, *Analyst*, 2005, 130(4): 545

92. X. Zhang, N. C. Shah, and R. P. Van Duyne, Sensitive and selective chem/bio sensing based on surface-enhanced Raman spectroscopy (SERS), *Vib. Spectrosc.*, 2006, 42(1): 2

93. G. Naja, P. Bouvrette, S. Hrapovic, and J. H. T. Luong, Raman-based detection of bacteria using silver nanoparticles conjugated with antibodies, *Analyst*, 2007, 132(7): 679

94. J. D. Driskell, K. M. Kwarta, R. J. Lipert, M. D. Porter, J. D. Neill, and J. F. Ridpath, Low-level detection of viral pathogens by a surface-enhanced Raman scattering based immunoassay, *Anal. Chem.*, 2005, 77(19): 6147

95. S. Shanmukh, L. Jones, J. Driskell, Y. Zhao, R. Dluhy, and R. A. Tripp, Rapid and sensitive detection of respiratory virus molecular signatures using a silver nanorod array SERS substrate, *Nano Lett.*, 2006, 6(11): 2630

96. Y. C. Cao, R. Jin, J. M. Nam, C. S. Thaxton, and C. A. Mirkin, Raman dye-labeled nanoparticle probes for proteins, *J. Am. Chem. Soc.*, 2003, 125(48): 14676

97. J. Johanson, K. Abravaya, W. Caminiti, D. Erickson, R. Flanders, G. Leckie, E. Marshall, C. Mullen, Y. Ohhashi, R. Perry, J. Ricci, J. Salituro, A. Smith, N. Tang, M. Vi, and J. Robinson, A new ultrasensitive assay for quantitation of HIV-1 RNA in plasma, *J. Virol. Methods*, 2001, 95(1–2): 81

98. S. M. H. Abanto, M. H. Hirata, R. D. C. Hirata, E. M. Mamizuka, M. Schmal, and S. Hoshino-Shimizu, Evaluation of Henes-PCR assay for Mycobacterium detection in different clinical specimens from patients with or without tuberculosis-associated HIV infection, *J. Clin. Lab. Anal.*, 2000, 14(5): 238

Frontiers of Physics

99. N. R. Isola, D. L. Stokes, and T. Vo-Dinh, Surface-enhanced Raman gene probe for HIV detection, *Anal. Chem.*, 1998, 70(7): 1352

100. For example: S. Weiss, Fluorescence spectroscopy of single biomolecules, *Science*, 1999, 283(5408): 1676

101. M. Osumi, The ultrastructure of yeast: Cell wall structure and formation, *Micron*, 1998, 29(2–3): 207

102. E. Podstawka and L. M. Proniewicz, Resonance Raman study of deoxy and ligated (O_2 and CO) mesoheme IX-reconstituted myoglobin, hemoglobin and its alpha and beta subunits, *J. Inorg. Biochem.*, 2004, 98(9): 1502

103. Y. Jin, M. Nagai, Y. Nagai, S. Nagatomo, and T. Kitagawa, Heme structures of five variants of hemoglobin M probed by resonance Raman spectroscopy, *Biochemistry*, 2004, 43(26): 8517

104. D. Wang and T. G. Spiro, Structure changes in hemoglobin upon deletion of C-terminal residues, monitored by resonance Raman spectroscopy, *Biochemistry*, 1998, 37(28): 9940

105. V. Jayaraman, K. R. Rodgers, I. Mukerji, and T. G. Spiro, Hemoglobin allostery: Resonance Raman spectroscopy of kinetic intermediates, *Science*, 1995, 269(5232): 1843

106. P. Etchegoin, H. Liem, R. C. Maher, L. F. Cohen, R. J. C. Brown, M. J. T. Milton, and J. C. Gallop, Observation of dynamic oxygen release in hemoglobin using surface enhanced Raman scattering, *Chem. Phys. Lett.*, 2003, 367(1–2): 223

107. T. G. Spiro and T. C. Strekas, Resonance Raman spectra of heme proteins: Effects of oxidation and spin state, *J. Am. Chem. Soc.*, 1974, 96(2): 338

108. I. P. Torres Filho, J. Terner, R. N. Pittman, E. Proffitt, and K. R. Ward, Measurement of hemoglobin oxygen saturation using Raman microspectroscopy and 532-nm excitation, *J. Appl. Physiol.*, 2008, 104(6): 1809

109. S. E. Bell and N. M. Sirimuthu, Surface-enhanced Raman spectroscopy (SERS) for sub-micromolar detection of DNA/RNA mononucleotide, *J. Am. Chem. Soc.*, 2006, 128(49): 15580

110. E. Bailo, L. Fruk, C. M. Niemeyer, and V. Deckert, Surface-enhanced Raman scattering as a tool to probe cytochrome P450-catalysed substrate oxidation, *Anal. Bioanal. Chem.*, 2009, 394(7): 1797

111. K. Niki, Y. Kawasaki, Y. Kimura, Y. Higuchi, and N. Yasuoka, Surface-enhanced Raman scattering of cytochromes c3 adsorbed on silver electrode and their redox behavior, *Langmuir*, 1987, 3(6): 982

112. D. A. Stuart, J. M. Yuen, N. Shah, O. Lyandres, C. R. Yonzon, M. R. Glucksberg, J. T. Walsh, and R. P. Van Duyne, In vivo glucose measurement by surface-enhanced Raman spectroscopy, *Anal. Chem.*, 2006, 78(20): 7211

113. O. Lyandres, J. M. Yuen, N. C. Shah, R. P. Van Duyne, J. T. Walsh, Jr., and M. R. Glucksberg, Progress toward an in vivo surface-enhanced Raman spectroscopy glucose sensor, *Diabetes Technology & Therapeutics*, 2008, 10(4): 257

114. J. P. Camden, J. A. Dieringer, J. Zhao, and R. P. Van Duyne, Controlled plasmonic nanostructures for surface-enhanced spectroscopy and sensing, *Acc. Chem. Res.*, 2008, 41(12): 1653

115. M. Iga, N. Kakuryu, T. Tanaami, J. Sajiki, K. Isozaki, and T. Itoh, Development of thin-film tunable band-pass filters based hyper-spectral imaging system applied for both surface enhanced Raman scattering and plasmon resonance Rayleigh scattering, *Rev. Sci. Instrum.*, 2012, 83(10): 103707

46

Yuko S. Yamamoto, et al., Front. Phys., 2014, 9(1)